

Bit-Interleaved Coded Multiple Beamforming with Perfect Coding

Boyu Li and Ender Ayanoglu

Center for Pervasive Communications and Computing

Department of Electrical Engineering and Computer Science

The Henry Samueli School of Engineering

University of California, Irvine

Irvine, California 92697-2625

Email: boyul@uci.edu, ayanoglu@uci.edu

Abstract

When the Channel State Information (CSI) is known by the transmitter as well as the receiver, beamforming techniques that employ Singular Value Decomposition (SVD) are commonly used in Multiple-Input Multiple-Output (MIMO) systems. In the absence of channel coding, when a single symbol is transmitted, these systems achieve the full diversity order provided by the channel. Whereas, this property is lost when multiple symbols are simultaneously transmitted. Full diversity can be restored when channel coding is added, as long as the code rate R_c and the number of employed subchannels S satisfy the condition $R_c S \leq 1$. By adding a properly designed constellation precoder, full diversity can be achieved for both uncoded and convolutional coded SVD systems, e.g., Fully Precoded Multiple Beamforming (FPMB) and Bit-Interleaved Coded Multiple Beamforming with Full Precoding (BICMB-FP) without the condition $R_c S \leq 1$. Recently discovered Perfect Space-Time Block Code (PSTBC) is a full-rate full-diversity space-time code, which achieves maximum coding gain for MIMO systems. Particular PSTBCs, which yield increased coding gain, only exist in dimensions 2, 3, 4 and 6. Previously, Perfect Coded Multiple Beamforming (PCMB) was proposed. PCMB transmits PSTBCs through uncoded multiple beamforming. It was shown that PCMB achieves the full diversity order and its performance is close to general MIMO systems using PSTBCs and FPMB, whereas the worst-case decoding complexity is significantly less than general MIMO systems using PSTBCs and is much lower than FPMB for dimensions 2 and 4. In this paper, a new technique, Bit-Interleaved Coded Multiple Beamforming with Perfect Coding (BICMB-PC), is introduced. BICMB-PC transmits PSTBCs through convolutional coded SVD systems. Simulation results show that BICMB-PC achieves almost the same

performance as BICMB-FP. Moreover, since the real and imaginary parts of the received signal can be separated for BICMB-PC of dimensions 2 and 4, and only the part corresponding to the coded bit is required to acquire one bit metric for the Viterbi decoder, BICMB-PC provides much lower decoding complexity than BICMB-FP.

I. INTRODUCTION

Substantial research and development has been carried out on Multiple-Input Multiple-Output (MIMO) systems, because they offer high spectral efficiency and performance in a given bandwidth. In such systems, space-time coding can be employed to offer spatial diversity, and increasingly, spatial multiplexing gains [1].

When Channel State Information (CSI) is available at the transmitter, beamforming techniques, which exploit Singular Value Decomposition (SVD), are applied in a MIMO system to achieve spatial multiplexing and thereby increase the data rate, or to enhance the performance [2]. However, spatial multiplexing without channel coding results in the loss of the full diversity order [3]. To overcome the diversity degradation, Bit-Interleaved Coded Multiple Beamforming (BICMB), which interleaves the codewords through the multiple subchannels, was proposed [4], [5]. BICMB can achieve the full diversity order as long as the code rate R_c and the number of employed subchannels S satisfy the condition $R_c S \leq 1$ [6], [7]. In [8], [9], [10], it was shown that by employing the constellation precoding technique, the full diversity order can be achieved for both uncoded and convolutional coded SVD systems, e.g., Fully Precoded Multiple Beamforming (FPMB) and Bit-Interleaved Coded Multiple Beamforming with Full Precoding (BICMB-FP) without the condition $R_c S \leq 1$.

In [11], the Perfect Space-Time Block Code (PSTBC) was introduced for dimensions 2, 3, 4, and 6. PSTBCs have the full rate, the full diversity, nonvanishing minimum determinant for increasing spectral efficiency, uniform average transmitted energy per antenna, and good shaping of the constellation. In [12], PSTBCs were generalized to any dimension. However, it was proved in [13] that particular PSTBCs, yielding increased coding gain, only exist in dimensions 2, 3, 4, and 6. Due to the advantages of PSTBCs, the Golden Code (GC), which is the best known PSTBC for MIMO systems with two transmit and two receive antennas [14], [15], has been incorporated into the 802.16e WiMAX standard [16].

In our previous work [17], [18], Perfect Coded Multiple Beamforming (PCMB) was proposed. PCMB combines PSTBCs with multiple beamforming and achieves the full rate and the full diversity, in a similar fashion to the general MIMO systems employing PSTBCs and FPMB. It was shown that for dimensions 2 and 4, all these three techniques have close Bit Error Rate (BER) performance, while the worst-case

decoding complexity of PCMB is significantly less than general MIMO systems using PSTBCs and is much lower than FPMB.

In this paper, a new technique with the full diversity order for convolutional coded SVD systems, called Bit-Interleaved Coded Multiple Beamforming with Perfect Coding (BICMB-PC), is proposed. BICMB-PC transmits bit-interleaved codewords of PSTBC through the multiple subchannels. Simulation results show that BICMB-PC achieves almost the same BER performance as BICMB-FP. Moreover, BICMB-PC has much lower complexity than BICMB-FP for dimensions 2 and 4, because the real and imaginary parts of the received signal can be separated, and only the part corresponding to the coded bit is required to calculate one bit metric for the Viterbi decoder.

The remainder of this paper is organized as follows: In Section II, the description of BICMB-PC is given. In Section III, the diversity analysis of BICMB-PC is provided. In Section IV, the decoding technique and complexity of BICMB-PC are shown. In Section V, performance comparisons of BICMB-PC and BICMB-FP are carried out. Finally, a conclusion is provided in Section VI.

II. BICMB-PC OVERVIEW

The structure of BICMB-PC is presented in Fig. 1. First, the convolutional encoder of code rate R_c , possibly combined with a perforation matrix for a high rate punctured code, generates the bit codeword \mathbf{c} from the information bits. Then, a random bit-interleaver is applied to generate the interleaved bit sequence, which is then modulated by M -QAM or M -HEX [19] and mapped by Gray encoding. Then S^2 consecutive complex-valued scalar symbols are encoded into one PSTBC codeword, where $S \in \{2, 3, 4, 6\}$ is the system dimension. Hence, at the k^{th} time instant, the PSTBC codeword \mathbf{Z}_k is constructed as

$$\mathbf{Z}_k = \sum_{v=1}^S \text{diag}(\mathbf{G}\mathbf{x}_{v,k})\mathbf{E}^{v-1} \quad (1)$$

where \mathbf{G} is an $S \times S$ unitary matrix, $\mathbf{x}_{v,k}$ is an $S \times 1$ vector whose elements are the v^{th} S input modulated scalar symbols, and

$$\mathbf{E} = \begin{bmatrix} 0 & 1 & \cdots & 0 & 0 \\ 0 & 0 & 1 & \cdots & \vdots \\ \vdots & \vdots & \ddots & \ddots & \vdots \\ 0 & \cdots & \cdots & \cdots & 1 \\ g & 0 & \cdots & 0 & 0 \end{bmatrix},$$

with

$$g = \begin{cases} i, & S = 2, 4, \\ e^{\frac{2\pi i}{3}}, & S = 3, \\ -e^{\frac{2\pi i}{3}}, & S = 6, \end{cases}$$

and $\text{diag}(\mathbf{w} = [w_1, \dots, w_S]^T)$ denotes a diagonal matrix with diagonal entries w_1, \dots, w_S . The selection of the \mathbf{G} matrix for different dimensions can be found in [11].

The MIMO channel $\mathbf{H} \in \mathbb{Z}^{N_r \times N_t}$ is assumed to be quasi-static, Rayleigh, and flat fading, and known by both the transmitter and the receiver, where $N_r = N_t = S$ denote the number of transmit and receive antennas respectively, and \mathbb{Z} stands for the set of complex numbers. The beamforming vectors are determined by the SVD of the MIMO channel, i.e., $\mathbf{H} = \mathbf{U}\mathbf{\Lambda}\mathbf{V}^H$, where \mathbf{U} and \mathbf{V} are unitary matrices, and $\mathbf{\Lambda}$ is a diagonal matrix whose s^{th} diagonal element, $\lambda_s \in \mathbb{R}^+$, is a singular value of \mathbf{H} in decreasing order, where \mathbb{R}^+ denotes the set of positive real numbers. When S streams are transmitted at the same time, the first S vectors of \mathbf{U} and \mathbf{V} are chosen to be used as beamforming matrices at the receiver and the transmitter, respectively.

The received signal at the k^{th} time instant is

$$\mathbf{Y}_k = \mathbf{\Lambda}\mathbf{Z}_k + \mathbf{N}_k, \quad (2)$$

where \mathbf{Y}_k is an $S \times S$ complex-valued matrix, and \mathbf{N}_k is the $S \times S$ complex-valued additive white Gaussian noise matrix whose elements have zero mean and variance $N_0 = S/\text{SNR}$. The channel matrix \mathbf{H} is complex Gaussian with zero mean and unit variance. The total transmitted power is scaled as S in order to make the received Signal-to-Noise Ratio (SNR) SNR .

The location of the coded bit $c_{k'}$ within the PSTBC codeword sequence is denoted as $k' \rightarrow (k, (m, n), j)$, where k , (m, n) , and j are the time instant of the PSTBC codewords, the symbol position in $\mathbf{X}_k = [\mathbf{x}_{1,k}, \dots, \mathbf{x}_{S,k}]$, and the bit position on the label of the scalar symbol $x_{(m,n),k}$, respectively. Let χ denote the signal set of the modulation scheme, and let χ_b^j denote a subset of χ whose labels have $b \in \{0, 1\}$ in the j^{th} bit position. By using the location information and the input-output relation in (2), the receiver calculates the Maximum Likelihood (ML) bit metrics for $c_{k'}$ as

$$\gamma^{(m,n),j}(\mathbf{Y}_k, c_{k'}) = \min_{x_{(m,n)} \in \chi_b^j} \|\mathbf{Y}_k - \mathbf{\Lambda}\mathbf{Z}\|^2. \quad (3)$$

Finally, the ML decoder, which uses Viterbi decoding, makes decisions according to the rule

$$\hat{\mathbf{c}} = \arg \min_{\mathbf{c}} \sum_{k'} \gamma^{(m,n),j}(\mathbf{Y}_k, c_{k'}). \quad (4)$$

III. DIVERSITY ANALYSIS

Based on the bit metrics in (3), the instantaneous Pairwise Error Probability (PEP) between the transmitted codeword \mathbf{c} and the decoded codeword $\hat{\mathbf{c}}$ is

$$\Pr(\mathbf{c} \rightarrow \hat{\mathbf{c}} | \mathbf{H}) = \Pr \left(\sum_{k'} \min_{x(m,n) \in \mathcal{X}_{c_{k'}}^j} \|\mathbf{Y}_k - \Lambda \mathbf{Z}\|^2 \geq \sum_{k'} \min_{x(m,n) \in \mathcal{X}_{\hat{c}_{k'}}^j} \|\mathbf{Y}_k - \Lambda \mathbf{Z}\|^2 | \mathbf{H} \right), \quad (5)$$

where $c_{k'}$ and $\hat{c}_{k'}$ are the coded bit of \mathbf{c} and $\hat{\mathbf{c}}$, respectively. Let d_H denote the Hamming distance between \mathbf{c} and $\hat{\mathbf{c}}$. It is assumed that the d_H coded bits are interleaved such that they are placed in $d \leq d_H$ distinct PSTBC codewords. Since the bit metrics corresponding to the same coded bits between the pairwise errors are the same, (5) is rewritten as

$$\Pr(\mathbf{c} \rightarrow \hat{\mathbf{c}} | \mathbf{H}) = \Pr \left(\sum_{k',d} \min_{x(m,n) \in \mathcal{X}_{c_{k'}}^j} \|\mathbf{Y}_k - \Lambda \mathbf{Z}\|^2 \geq \sum_{k',d} \min_{x(m,n) \in \mathcal{X}_{\hat{c}_{k'}}^j} \|\mathbf{Y}_k - \Lambda \mathbf{Z}\|^2 | \mathbf{H} \right), \quad (6)$$

where $\sum_{k',d}$ stands for the summation of the d values corresponding to the different coded bits between the bit codewords.

Define $\tilde{\mathbf{Z}}_k$ and $\hat{\mathbf{Z}}_k$ as

$$\begin{aligned} \tilde{\mathbf{Z}}_k &= \arg \min_{x(m,n) \in \mathcal{X}_{c_{k'}}^j} \|\mathbf{Y}_k - \Lambda \mathbf{Z}\|^2, \\ \hat{\mathbf{Z}}_k &= \arg \min_{x(m,n) \in \mathcal{X}_{\hat{c}_{k'}}^j} \|\mathbf{Y}_k - \Lambda \mathbf{Z}\|^2, \end{aligned} \quad (7)$$

where $\bar{c}_{k'}$ is the complement of $c_{k'}$ in binary. It is easily found that $\tilde{\mathbf{Z}}_k$ is different from $\hat{\mathbf{Z}}_k$ since the sets that $x(m,n)$'s belong to are disjoint, as can be seen from the definition of $\mathcal{X}_{c_{k'}}^j$. In the same manner, it is clear that \mathbf{Z}_k is different from $\hat{\mathbf{Z}}_k$. With $\tilde{\mathbf{Z}}_k$ and $\hat{\mathbf{Z}}_k$, (6) is rewritten as

$$\Pr(\mathbf{c} \rightarrow \hat{\mathbf{c}} | \mathbf{H}) = \Pr \left(\sum_{k',d} \|\mathbf{Y}_k - \Lambda \tilde{\mathbf{Z}}\|^2 \geq \sum_{k',d} \|\mathbf{Y}_k - \Lambda \hat{\mathbf{Z}}\|^2 \right). \quad (8)$$

Based on the fact that $\|\mathbf{Y}_k - \Lambda \mathbf{Z}\|^2 \geq \|\mathbf{Y}_k - \Lambda \tilde{\mathbf{Z}}\|^2$ and the relation in (2), equation (8) is upper-bounded

by

$$\Pr(\mathbf{c} \rightarrow \hat{\mathbf{c}} \mid \mathbf{H}) \leq \Pr\left(\xi \geq \sum_{k',d} \|\mathbf{\Lambda}(\mathbf{Z}_k - \hat{\mathbf{Z}}_k)\|^2\right), \quad (9)$$

where $\xi = \sum_{k',d} \text{Tr}[-(\mathbf{Z}_k - \hat{\mathbf{Z}}_k)^H \mathbf{\Lambda}^H \mathbf{N}_k - \mathbf{N}_k^H \mathbf{\Lambda}(\mathbf{Z}_k - \hat{\mathbf{Z}}_k)]$. Since ξ is a zero-mean Gaussian random variable with variance $2N_0 \sum_{k',d} \|\mathbf{\Lambda}(\mathbf{Z}_k - \hat{\mathbf{Z}}_k)\|^2$, (9) is replaced by the Q function as

$$\Pr(\mathbf{c} \rightarrow \hat{\mathbf{c}} \mid \mathbf{H}) = Q\left(\sqrt{\frac{\sum_{k',d} \|\mathbf{\Lambda}(\mathbf{Z}_k - \hat{\mathbf{Z}}_k)\|^2}{2N_0}}\right). \quad (10)$$

By using the upper bound on the Q function $Q(x) \leq \frac{1}{2}e^{-x^2/2}$, the average PEP can be upper bounded as

$$\begin{aligned} \Pr(\mathbf{c} \rightarrow \hat{\mathbf{c}}) &= E[\Pr(\mathbf{c} \rightarrow \hat{\mathbf{c}} \mid \mathbf{H})] \\ &\leq E\left[\frac{1}{2} \exp\left(-\frac{\sum_{k',d} \|\mathbf{\Lambda}(\mathbf{Z}_k - \hat{\mathbf{Z}}_k)\|^2}{4N_0}\right)\right]. \end{aligned} \quad (11)$$

In [17], [18], it was shown that

$$\begin{aligned} \|\mathbf{\Lambda}\mathbf{Z}_k\|^2 &= \text{Tr}[\mathbf{Z}_k^H \mathbf{\Lambda}^H \mathbf{\Lambda}\mathbf{Z}_k] \\ &= \sum_{u=1}^S \lambda_u^2 \sum_{v=1}^S |\mathbf{g}_u^T \mathbf{x}_{v,k}|^2, \end{aligned} \quad (12)$$

where \mathbf{g}_u^T denotes the u^{th} row of \mathbf{G} . By replacing \mathbf{Z}_k in (12) by $\mathbf{Z}_k - \hat{\mathbf{Z}}_k$, (11) is then rewritten as

$$\begin{aligned} \Pr(\mathbf{c} \rightarrow \hat{\mathbf{c}}) &\leq E\left[\frac{1}{2} \exp\left(-\frac{\sum_{k',d} \sum_{u=1}^S \lambda_u^2 \tau_u}{4N_0}\right)\right] \\ &= E\left[\frac{1}{2} \exp\left(-\frac{\sum_{u=1}^S \lambda_u^2 \sum_{k',d} \tau_u}{4N_0}\right)\right], \end{aligned} \quad (13)$$

where $\tau_u = \sum_{v=1}^S |\mathbf{g}_u^T(\mathbf{x}_{v,k} - \hat{\mathbf{x}}_{v,k})|^2$. The upper bound in (13) can be further bounded by employing a theorem from [20] which is given below.

Theorem 1: Consider the largest $S \leq \min(N_t, N_r)$ eigenvalues μ_s of the uncorrelated central $N_r \times N_t$ Wishart matrix that are sorted in decreasing order, and a weight vector $\boldsymbol{\rho} = [\rho_1, \dots, \rho_S]^T$ with non-negative real elements. In the high SNR regime, an upper bound for the expression $E[\exp(-\gamma \sum_{s=1}^S \rho_s \mu_s)]$, which

is used in the diversity analysis of a number of MIMO systems, is

$$E \left[\exp \left(-\gamma \sum_{s=1}^S \rho_s \mu_s \right) \right] \leq \zeta (\rho_{\min} \gamma)^{-(N_r - \delta + 1)(N_t - \delta + 1)},$$

where γ is signal-to-noise ratio, ζ is a constant, $\rho_{\min} = \min_{\rho_i \neq 0} \{\rho_i\}_{i=1}^S$, and δ is the index to the first non-zero element in the weight vector.

Proof: See [20]. ■

Note that $\tau_u > 0$, then $\delta = 1$. By applying Theorem 1 to (13), an upper bound of PEP is

$$\Pr(\mathbf{c} \rightarrow \hat{\mathbf{c}}) \leq \zeta \left(\frac{\min\{\sum_{k',d} \tau_u\}}{4N} SNR \right)^{-N_r N_t}. \quad (14)$$

Hence, BICMB-PC achieves the full diversity order.

IV. DECODING

It was shown in [17], [18], that each element of $\Lambda \mathbf{Z}_k$ in (2) is related to only one of the $\mathbf{x}_{v,k}$. Consequently, the elements of $\Lambda \mathbf{Z}_k$ can be divided into S groups, where the v^{th} group contains elements related to $\mathbf{x}_{v,k}$, and $v = 1, \dots, S$.

Take GC ($S = 2$) as an example,

$$\Lambda \mathbf{Z}_k = \begin{bmatrix} \lambda_1 \mathbf{g}_1^T \mathbf{x}_{1,k} & \lambda_1 \mathbf{g}_1^T \mathbf{x}_{2,k} \\ i \lambda_2 \mathbf{g}_2^T \mathbf{x}_{2,k} & \lambda_2 \mathbf{g}_2^T \mathbf{x}_{2,k} \end{bmatrix}. \quad (15)$$

The input-output relation in (2) is then decomposed into two equations as

$$\begin{aligned} \check{\mathbf{y}}_{1,k} &= \begin{bmatrix} Y_{(1,1),k} \\ Y_{(2,2),k} \end{bmatrix} = \begin{bmatrix} \lambda_1 \mathbf{g}_1^T \mathbf{x}_{1,k} \\ \lambda_2 \mathbf{g}_2^T \mathbf{x}_{1,k} \end{bmatrix} + \begin{bmatrix} N_{(1,1),k} \\ N_{(2,2),k} \end{bmatrix}, \\ \check{\mathbf{y}}_{2,k} &= \begin{bmatrix} Y_{(1,2),k} \\ Y_{(2,1),k} \end{bmatrix} = \begin{bmatrix} \lambda_1 \mathbf{g}_1^T \mathbf{x}_{2,k} \\ i \lambda_2 \mathbf{g}_2^T \mathbf{x}_{2,k} \end{bmatrix} + \begin{bmatrix} N_{(1,2),k} \\ N_{(2,1),k} \end{bmatrix}, \end{aligned} \quad (16)$$

where $Y_{(m,n),k}$ and $N_{(m,n),k}$ denote the $(m, n)^{\text{th}}$ element of \mathbf{Y}_k and \mathbf{N}_k respectively. Let $\check{\mathbf{n}}_{1,k} = [N_{(1,1),k}, N_{(2,2),k}]^T$ and $\check{\mathbf{n}}_{2,k} = [N_{(1,2),k}, N_{(2,1),k}]^T$, then (16) can be further rewritten as

$$\begin{aligned} \check{\mathbf{y}}_{1,k} &= \Lambda \mathbf{G} \mathbf{x}_{1,k} + \check{\mathbf{n}}_{1,k}, \\ \check{\mathbf{y}}_{2,k} &= \Phi \Lambda \mathbf{G} \mathbf{x}_{2,k} + \check{\mathbf{n}}_{2,k}, \end{aligned} \quad (17)$$

where

$$\Phi = \begin{bmatrix} 1 & 0 \\ 0 & i \end{bmatrix}.$$

A similar procedure can be applied to larger dimensions. Then in general, the received signal, which is divided into S parts, can be represented as

$$\check{\mathbf{y}}_{v,k} = \Phi_v \Lambda \mathbf{G} \mathbf{x}_{v,k} + \check{\mathbf{n}}_{v,k}, \quad (18)$$

where $v = 1, \dots, S$ and $\Phi_v = \text{diag}(\phi_{v,1}, \dots, \phi_{v,S})$ is a diagonal unitary matrix whose elements satisfy

$$\phi_{v,u} = \begin{cases} 1, & 1 \leq u \leq S + 1 - v, \\ g, & S + 2 - v \leq u \leq S. \end{cases}$$

By using the QR decomposition of $\Lambda \mathbf{G} = \mathbf{Q} \mathbf{R}$, where \mathbf{R} is an upper triangular matrix, and the matrix \mathbf{Q} is unitary, and moving $\Phi_v \mathbf{Q}$ to the left hand, (18) is rewritten as

$$\tilde{\mathbf{y}}_{v,k} = \mathbf{Q}^H \Phi_v^H \check{\mathbf{y}}_{v,k} = \mathbf{R} \mathbf{x}_{v,k} + \mathbf{Q}^H \Phi_v^H \check{\mathbf{n}}_{v,k} = \mathbf{R} \mathbf{x}_{v,k} + \tilde{\mathbf{n}}_{v,k}. \quad (19)$$

Then the ML bit metrics in (3) can be simplified as

$$\gamma^{(m,n),j}(\mathbf{Y}_k, c_{k'}) = \min_{\mathbf{x} \in \xi_{c_{k'}}^{n,j}} \|\tilde{\mathbf{y}}_{m,k} - \mathbf{R} \mathbf{x}\|^2, \quad (20)$$

where $\xi_{c_{k'}}^{n,j}$ is a subset of χ^S , defined as

$$\xi_b^{n,j} = \{\mathbf{x} = [x_1 \cdots x_S]^T : x_{s|s=n} \in \chi_b^j, \text{ and } x_{s|s \neq n} \in \chi\}.$$

The simplified ML bit metrics (20) are similar to BICMB-FP presented in [9], [10], which are used to calculate $\frac{1}{2}M^S$ points by exhaustive search for one bit metric. Hence, the complexity is proportional to M^S , denoted by $\mathcal{O}(M^S)$. Sphere Decoding (SD) is an alternative for ML with reduced complexity [21], which reduces the average complexity and provides the worst-case complexity of $\mathcal{O}(M^S)$.

Particularly, it was shown in [17], [18], that \mathbf{R} is a real-valued matrix for dimensions 2 and 4, which implies that the real and imaginary parts of $\tilde{\mathbf{y}}_{m,k}$ in (20) can be separated, and only the part corresponding to the coded bit is required for calculating one bit metric of the Viterbi decoder. Assume that square M -QAM is used, whose real and imaginary parts are Gray coded separately as two \sqrt{M} -PAM. Therefore,

the ML bit metrics in (20) can be further simplified for dimensions 2 and 4 as

$$\gamma^{(m,n),j}(\mathbf{Y}_k, c_{k'}) = \min_{\Re[\mathbf{x}] \in \Re[\xi_{c_{k'}}^{n,j}]} \|\Re[\tilde{\mathbf{y}}_{m,k}] - \mathbf{R}\Re[\mathbf{x}]\|^2, \quad (21)$$

if $c_{k'}$ is mapped to the real part, or

$$\gamma^{(m,n),j}(\mathbf{Y}_k, c_{k'}) = \min_{\Im[\mathbf{x}] \in \Im[\xi_{c_{k'}}^{n,j}]} \|\Im[\tilde{\mathbf{y}}_{m,k}] - \mathbf{R}\Im[\mathbf{x}]\|^2, \quad (22)$$

if $c_{k'}$ is mapped to the imaginary part, where $\Re[\mathbf{x}]$ and $\Im[\mathbf{x}]$ denote the real and imaginary parts of \mathbf{x} respectively. For (21) and (22), the worst-case decoding complexity is only $\mathcal{O}(M^{\frac{S}{2}})$, which is much lower than BICMB-FP.

V. SIMULATION RESULTS

In this section, simulation results are provided for BICMB-PC and BICMB-FP of dimensions 2 and 4 for different modulation schemes, since BICMB-PC has much lower decoding complexity than BICMB-FP in these dimensions.

Considering $R_c = 2/3$, 2×2 systems, Fig. 2 shows BER-SNR performance comparison of BICMB-PC and BICMB-FP. The constellation precoder for FPMB is selected as the best one introduced in [8]. Simulation results show that BICMB-PC and BICMB-FP, with the worst-case decoding complexity of $\mathcal{O}(M)$ and $\mathcal{O}(M^2)$ to acquire one bit metric respectively, achieve almost the same performance for all of 4-QAM, 16-QAM, and 64-QAM.

In the case of $R_c = 4/5$, 4×4 systems, Fig. 3 shows BER-SNR performance comparison of BICMB-PC and BICMB-FP for 4-QAM and 16-QAM. The constellation precoder for FPMB is also chosen as the best one in [8]. Similarly, simulation results show that BICMB-PC achieves almost the same performance as BICMB-FP. Moreover, the worst-case decoding complexity of $\mathcal{O}(M^2)$ to get one bit metric for BICMB-PC is much lower than that of $\mathcal{O}(M^4)$ for BICMB-FP.

VI. CONCLUSION

In this paper, BICMB-PC which combines PSTBC and multiple beamforming technique is proposed. It is shown that PSTBC achieves the full diversity order, and a similar BER performance to BICMB-FP, which is also a full-diversity technique for convolutional coded SVD systems. Particularly, for dimensions 2 and 4, because only one of the real or imaginary part of the received signal is required to calculate one

bit metric for the Viterbi decoder, the worst-case decoding complexity of BICMB-PC is much lower than BICMB-FP, which provides the advantage of BICMB-PC.

REFERENCES

- [1] V. Tarokh, N. Seshadri, and A. R. Calderbank, "Space-Time Codes for High Data Rate Wireless Communication: Performance Criterion and Code Construction," *IEEE Trans. Inf. Theory*, vol. 44, no. 2, pp. 744–765, Mar. 1998.
- [2] H. Jafarkhani, *Space-Time Coding: Theory and Practice*. Cambridge University Press, 2005.
- [3] E. Sengul, E. Akay, and E. Ayanoglu, "Diversity Analysis of Single and Multiple Beamforming," *IEEE Trans. Commun.*, vol. 54, no. 6, pp. 990–993, Jun. 2006.
- [4] E. Akay, E. Sengul, and E. Ayanoglu, "Bit-Interleaved Coded Multiple Beamforming," *IEEE Trans. Commun.*, vol. 55, no. 9, pp. 1802–1811, Sep. 2007.
- [5] E. Akay, H. J. Park, and E. Ayanoglu. (2008) On "Bit-Interleaved Coded Multiple Beamforming". arXiv: 0807.2464. [Online]. Available: <http://arxiv.org>
- [6] H. J. Park and E. Ayanoglu, "Diversity Analysis of Bit-Interleaved Coded Multiple Beamforming," in *Proc. IEEE ICC 2009*, Dresden, Germany, Jun. 2009, pp. 1–9.
- [7] —, "Diversity Analysis of Bit-Interleaved Coded Multiple Beamforming," *IEEE Trans. Commun.*, vol. 58, no. 8, pp. 2457–2463, Aug. 2010.
- [8] —, "Constellation Precoded Beamforming," in *Proc. IEEE Globecom 2009*, Honolulu, HI, USA, Nov. 2009, pp. 1–6.
- [9] —, "Bit-Interleaved Coded Multiple Beamforming with Constellation Precoding," in *Proc. IEEE ICC 2010*, Cape Town, South Africa, May 2010, pp. 1–6.
- [10] H. J. Park, B. Li, and E. Ayanoglu, "Multiple Beamforming with Constellation Precoding: Diversity Analysis and Sphere Decoding," in *Proc. IEEE ITA 2010*, San Diego, CA, USA, Apr. 2010, pp. 1–11.
- [11] F. Oggier, G. G. Rekaya, J.-C. Belfiore, and E. Viterbo, "Perfect Space-Time Block Codes," *IEEE Trans. Inf. Theory*, vol. 52, no. 9, pp. 3885–3902, 2006.
- [12] P. Elia, B. A. Sethuraman, and P. V. Kumar, "Perfect Space-Time Codes with Minimum and Non-Minimum Delay for any Number of Antennas," in *Proc. WIRELESSCOM 2005*, vol. 1, Sheraton Maui Resort, HI, USA, Jun. 2005, pp. 722–727.
- [13] G. Berhuy and F. Oggier, "On the Existence of Perfect Space-Time Codes," *IEEE Trans. Inf. Theory*, vol. 55, no. 5, pp. 2078–2082, May 2009.
- [14] J.-C. Belfiore, G. Rekaya, and E. Viterbo, "The Golden Code: a 2×2 Full-Rate Space-Time Code With Nonvanishing Determinants," *IEEE Trans. Inf. Theory*, vol. 51, pp. 1432–1436, Apr. 2005.
- [15] P. Dayal and M. K. Varanasi, "An Optimal two Transmit Antenna Space-Time Code and Its Stacked Extensions," *IEEE Trans. Inf. Theory*, vol. 51, no. 12, pp. 4348–4355, Dec. 2005.
- [16] *IEEE 802.16e-2005: IEEE Standard for Local and Metropolitan Area Network - Part 16: Air Interface for Fixed and Mobile Broadband Wireless Access Systems - Amendment 2: Physical Layer and Medium Access Control Layers for Combined Fixed and Mobile Operation in Licensed Bands*, Feb. 2006.
- [17] B. Li and E. Ayanoglu, "Golden Coded Multiple Beamforming," in *Proc. IEEE GLOBECOM 2010*, Miami, Florida, USA, Dec. 2010, to be published.
- [18] —. (2010) Golden Coded Multiple Beamforming. arXiv: 1009.0050. [Online]. Available: <http://arxiv.org>

- [19] G. J. Forney, R. Gallager, G. Lang, F. Longstaff, and S. Qureshi, "Efficient Modulation for Band-Limited Channels," *IEEE J. Sel. Areas Commun.*, vol. 2, no. 5, pp. 632–647, Sep. 1984.
- [20] H. J. Park and E. Ayanoglu, "An Upper Bound to the Marginal PDF of the Ordered Eigenvalues of Wishart Matrices and Its Application to MIMO Diversity Analysis," in *Proc. IEEE ICC 2010*, Cape Town, South Africa, May 2010, pp. 1–6.
- [21] J. Jaldén and B. Ottersten, "On the Complexity of Sphere Decoding in Digital Communications," *IEEE Trans. Signal Process.*, vol. 53, no. 4, pp. 1474–1484, Apr. 2005.

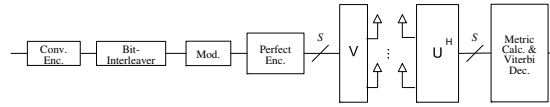


Fig. 1. Structure of BICMB-PC.

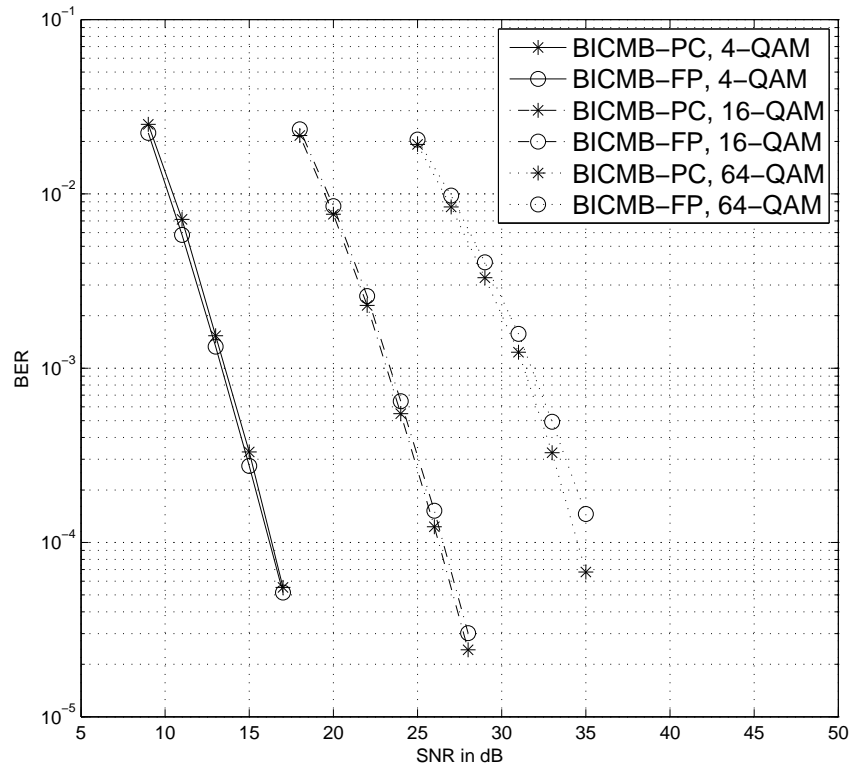


Fig. 2. BER vs. SNR for BICMB-PC and BICMB-FP for $R_c = 2/3$, 2×2 systems.

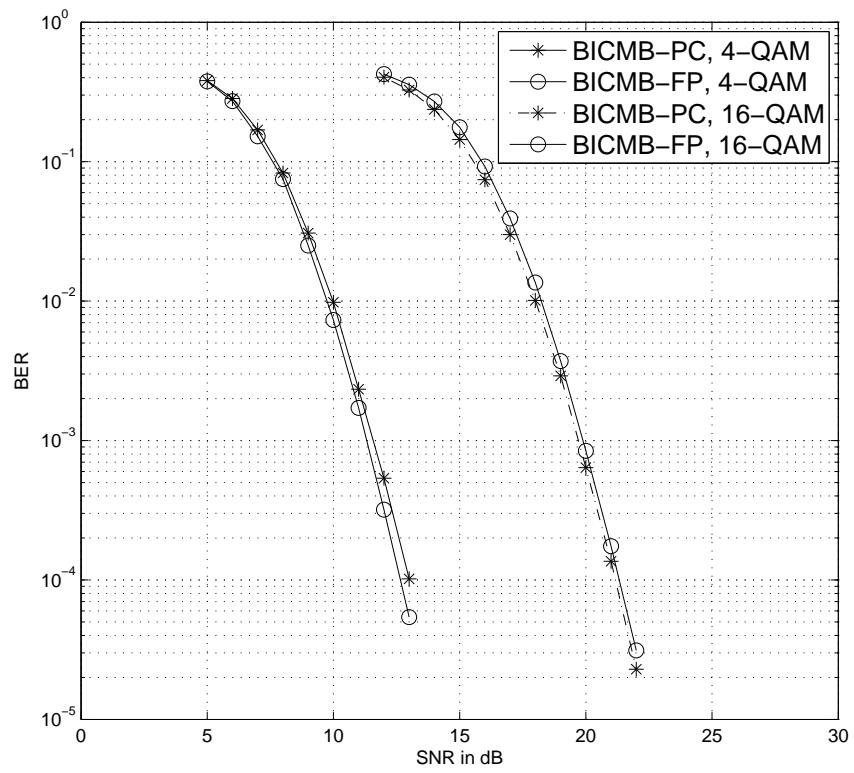


Fig. 3. BER vs. SNR for BICMB-PC and BICMB-FP for $R_c = 4/5$, 4×4 systems.